Comparison of heuristics and metaheuristics for topology optimisation in acoustic porous materials

Vivek T. Ramamoorthy,[1, a)] Ender Özcan,[1, b] Andrew J. Parkes,[1, c] Abhilash Sreekumar,[2, d] Luc Jaouen,[3, e] and François-Xavier Bécot[3, f]

[1] *Computational Optimisation and Learning Lab, School of Computer Science, University of Nottingham, NG8 1BB, United Kingdom*

[2] *Centre for Structural Engineering and Informatics, Faculty of Engineering, University of Nottingham, NG7 2RD, United Kingdom*

[3] *Matelys–Research Lab, 7 Rue des Maraîchers, Vaulx-en-Velin, 69120, France*

(Dated: 27 October 2021)

When designing sound packages, often fully filling the available space with acoustic materials is not the most absorbing solution. Better solutions can be obtained by creating cavities of air pockets, but determining the most optimal shape and topology that maximises sound absorption is a computationally challenging task. Many recent topology optimisation applications in acoustics use heuristic methods such as solid-isotropic-material-with-penalisation (SIMP) to quickly find near-optimal solutions. This study investigates seven heuristic and metaheuristic optimisation approaches including SIMP applied to topology optimisation of acoustic porous materials for absorption maximisation. The approaches tested are hill climbing, constructive heuristics, SIMP, genetic algorithm, tabu search, covariance-matrix-adaptation evolution strategy (CMA-ES), and differential evolution. All the algorithms are tested on seven benchmark problems varying in material properties, target frequencies, and dimensions. The empirical results show that hill climbing, constructive heuristics, and a discrete variant of CMA-ES outperform the other algorithms in terms of the average quality of solutions over the different problem instances. Though gradient-based SIMP algorithms converge to local optima in some problem instances, they are computationally more efficient. One of the general lessons is that different strategies explore different regions of the search space producing unique sets of solutions.

 [http://dx.doi.org/10.1121/10.0006784]

[Editor: Kirill V. Horoshenkov] Pages: 3164–3175

I. INTRODUCTION

A. Background

Historically, shape designs in engineering have been arrived at via a trial-and-error process, intuition, incremental improvements to old designs, human decision-making from numerical analyses, and recently, solely by computer analyses. Superior-to-human engineering designs have been achieved by computers using technologies such as structural topology optimisation. Topology optimisation involves finding the optimal topology (number of holes) and shape (size, dimensions) for a structure such that a given performance indicator is either maximised or minimised. Bendsøe and Kikuchi[1] introduced the concept of simultaneously optimising both shape and topology in the late 1980s. Since then, many theoretical developments have been made, and a community of researchers has actively been working in this field. One of the ways to formulate a topology optimisation problem is finding the optimal assignment of materials in each finite element of a discretised structure. In principle, this formulation is discrete optimisation, and finding the exact global optimum is computationally challenging. Exact optimisation techniques that guarantee to find the global optimum remain prohibitively expensive. Evaluating all possible solutions becomes impractical due to the large search space sizes and the expensive finite element evaluations. A noteworthy effort towards topology optimisation using an exact approach was by Stolpe and Bendsøe[2] on the Zhou and Rozvany problem instance[3]. But justifiably, the focus of previous work has mainly been on the inexact or *heuristic* optimisation approaches.

B. Heuristics

Heuristics are techniques that find solutions close-enough to the global optimum in reasonable time.

[a)] vivek.thaminniramamoorthy@nottingham.ac.uk
ORCID:0000-0002-1147-6579
[b)] ORCID: 0000-0003-0276-1391
[c)] ORCID: 0000-0002-8847-1856
[d)] ORCID: 0000-0003-2902-333X
[e)] ORCID: 0000-0002-3141-800X
[f)] ORCID: 0000-0001-6892-8436

Though heuristics do not guarantee to find the optimal solution, they are well-established and often the only viable option to address hard problems, such as those in NP-complete and NP-hard classes. The three most popular heuristic approaches applied to topology optimisation problems are solid-isotropic-material-with-penalisation(SIMP)[1,4–6], bi-directional evolutionary structural optimisation BESO[7–9], and the level-set method[10–12]. Among these, SIMP is the most commonly used and well-studied approach. In this approach, the discrete problem is relaxed to the continuous space by allowing intermediate materials between solid and void. A penalty-based material interpolation scheme is used to represent intermediate materials and a gradient-based optimisation strategies such as optimality criteria[13] or method of moving asymptotes[14] are used to move across the design variable space to find a near-optimal design. As SIMP is a derivative-based technique, it requires that a sensitivity analysis be carried out. BESO, not to be confused with evolutionary algorithms despite its name, is a type of constructive approach which iteratively adds material where stresses are high and removes material where stresses are low to arrive at a design. In the level-set method, a scalar field is associated with the design domain region and the isosurfaces of this scalar field are made the boundaries of the topology. This scalar field is then optimised to optimise the topology.

C. Metaheuristics

While heuristics are quick strategies to find near-optimal solutions, it was realised by Glover[15] that many powerful heuristic approaches follow certain higher-level guidelines. These guidelines can be considered heuristics to design heuristic algorithms, and hence are termed *meta*heuristics. A popular example of a metaheuristic is genetic algorithms, wherein the guideline is to initiate a population of solutions, apply selection pressure to pick good individuals, recombine the selected individuals, mutate them and replace them into the population. Numerous metaheuristic techniques, such as genetic algorithms and CMA-ES, have also been studied on structural topology optimisation problems[16,44].

D. Acoustic topology optimisation

Theoretical developments in structural topology optimisation have focused on the classical problem of compliance minimisation[18,19]. Nevertheless, the application of topology optimisation techniques to other problem domains is steadily on the rise[18,20,21]. These techniques have already been extended to acoustics, giving rise to a sub-field called acoustic topology optimisation.

At the time of writing this article, topology optimisation has been performed on a variety of acoustic applications, including horns, mufflers, rooms and sound barriers[22–36]. A majority of these applications use the gradient-based SIMP method or its variants, while a small fraction of them use BESO or level-set methods. These applications can be categorised into acoustic fluid-structure interaction problems and porous material problems. In acoustic fluid-structure interaction problems, the material choices are non-porous solid and fluid phases, and the wave propagation is modelled using mixed formulations[37,38]. Within acoustic fluid-structure interaction, problems other than topology optimisation such as material parameter estimation[39] have also found the application of gradient-based methods such as the method of moving asymptotes[40]. In porous material topology optimisation problems, the material choices also include poroelastic materials, and specialised Biot formulations[41,42] are generally used. In some applications[31,43], boundary element method is used to optimise the boundary topology instead of the bulk topology. In this article, poroelastic material topology optimisation is in focus. Specifically, we refer to topology optimisation in the context of finding optimal mesoscale shapes and topologies, i.e., on the order of magnitude of the material thickness, and not the optimisation of their microstructures.

Although metaheuristics have been previously tested on classical structural topology optimisation problems[16,44], their use has been limited in acoustic topology optimisation applications[17,45]. Only a few optimisation approaches have been tested, and optimisation theory exclusive to this problem domain remains yet to be explored. The present work is a step in this direction.

E. Contributions in this work

The goal of the present work is to investigate the performance of alternative heuristic optimisation approaches, including a few well-known metaheuristic approaches on a set of benchmark problems. In this article, the approaches compared are hill climbing, constructive heuristics, SIMP, genetic algorithms, tabu search, CMA-ES and differential evolution. While SIMP and its variants use gradients, none of the other approaches use any domain-specific information from the problem other than the objective function. Optimisation tests show how different approaches perform for various CPU time budgets. Notably, while SIMP algorithms produce good-quality solutions at low CPU time budgets, certain other algorithms such as hill climbing, constructive heuristics and CMA-ES outperform at higher computational budgets. The findings reported in this paper may serve as a useful prelude to develop better strategies for topology optimisation in acoustic porous materials.

The article is organised as follows: the optimisation problem description and the modelling methodology are given in Sec. II, concise descriptions and settings of the optimisation approaches are given in Sec. III, and the results from the optimisation tests are discussed in Sec. IV. Further, the pseudocodes of all algorithms, runtime comparisons, solution quality distributions, and final optimal shapes from all algorithms for all problem instances are included in the supplementary material.[60]

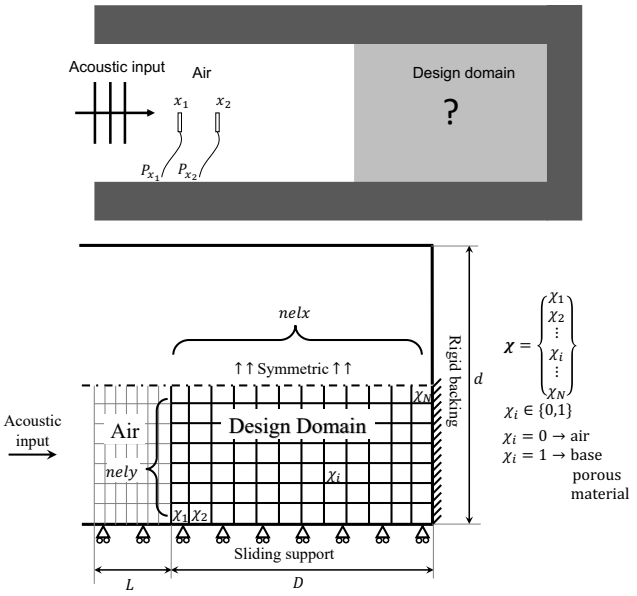

FIG. 1. Finite element model of an impedance tube system with the design domain where the shape and topology of a poroelastic material is to be optimised.

II. PROBLEM DESCRIPTION AND MODELLING

A. Maximising sound absorption in normal incidence

Consider the following problem: Given a finite element model of an impedance tube as shown in Figure 1, what is the best assignment of either air or a given poroelastic material to each element in the design domain that maximises the sound absorption of an acoustic source? The optimisation formulation can be written as:

$$\max_{\chi_i} \quad \overline{\alpha}(\boldsymbol{\chi}) = \frac{1}{n}\sum_{f=f_1}^{f_n} \alpha(\boldsymbol{\chi}, f) \tag{1}$$

$$\boldsymbol{\chi} : \chi_i \in \{0,1\} \quad \forall \quad i = 1, 2, \ldots, N$$
$$\overline{\alpha} \in [0,1]$$

where $\alpha(\boldsymbol{\chi}, f)$ is the sound absorption coefficient in normal incidence for a given shape $\boldsymbol{\chi}$ for frequency f, χ_i are the decision variables represent the choice between air and porous material for the i^{th} element, N is the number of elements in the design domain, and $f_1, f_2, ..., f_n$ are the target frequencies for which the mean absorption is to be maximised (where n is the number of frequencies considered). The symbol $\overline{\alpha}$ is used to refer to the mean sound absorption coefficient (α) across the target frequencies. In this paper, $\overline{\alpha}$ may be referred to as simply *absorption* or *fitness*, which is to be maximised.

Note that in Eq. (1), a volume fraction constraint is not included, which is unlike in usual topology optimisation problems. One reason is that in porous material topology optimisation, often the optimal shapes need to be carved out from a large block of the base porous material. The removed material may not often constitute material-saving, as the cost of recycling the carved out material could negate the material-saving benefit. Another reason is that more optimisation approaches to be tested as the formulation would resemble a conventional discrete optimisation problem. Without the volume constraint, since two choices are available (air or the base porous material) for each of the N elements in the design domain the search space size becomes 2^N . If a limit V_f is imposed on the ratio of porous volume to the total volume in the design domain ($\frac{1}{N}\sum_{i=1}^{N}\chi_i = V_f$), the search space size would become ${}^{N}C_{(V_f N)}$. In both these cases, the number of feasible solutions grows quickly with an increase in N. Since discrete optimisation is considered difficult to solve, the problem is usually relaxed to a continuous problem allowing χ_i to take values between 0 and 1, in other words allowing intermediate materials between air and porous material in the design domain. The problem is then solved using continuous optimisation approaches. Intermediate materials given by $\chi_i \in (0,1)$ are modelled using interpolating the material properties. One such interpolation scheme is the SIMP scheme (not to be confused with the SIMP approach). Using this scheme, the material property ψ for the intermediate material is given by Eq. (2).

$$\psi_i = \psi_{air} + \chi_i^p[\psi_{por} - \psi_{air}] \tag{2}$$

$$\psi \in \{E, \nu, \widetilde{\rho}, \widetilde{\gamma}_s, \widetilde{\rho}_{eq}, \widetilde{\mathrm{K}}_{eq}\} \tag{3}$$

Here, ψ is any material property from Young's modulus (E), Poisson's ratio (ν), modified Biot density ($\widetilde{\rho}$), coupling factor ($\widetilde{\gamma}_s$), dynamic mass density ($\widetilde{\rho}_{eq}$), dynamic bulk modulus ($\widetilde{\mathrm{K}}_{eq}$), etc. Though filtering techniques and interpolation penalties are used to enforce discrete solutions in such continuous formulations, often the resulting solutions tend to have intermediate materials, i.e., $\chi_i \in (0,1)$. Since filters in topology optimisation play a role in the optimisation performance, in this study no filters or manufacturability restrictions are considered—with the view that these can be done in post-processing.

B. Computing sound absorption and its gradients

To compute sound absorption, the poroelastic system constituting the fixed and design domains is modelled using the alternative Biot finite element formulations described by Bécot and Jaouen.[42] This formulation is based on the mixed $\{\mathbf{u}, \mathbf{P}\}$ formulation by Atalla *et al.*[41] The acoustic model for the fluid part is given by the Johnson-Champoux-Allard-Lafarge (JCAL) model.[46–48] To naturally account for the interface between porous and air regions, the unified analysis approach proposed and verified by Lee et al[24] is adopted. For intermediate material properties between air and porous material, the SIMP interpolation scheme[49] is used. The poroelastic system governing equations can be expressed in matrix form in

Eq. (4).

$$\underbrace{\begin{bmatrix} \tilde{\mathbf{K}} - \omega^2\tilde{\mathbf{M}} & -\tilde{\mathbf{C}} \\ -\tilde{\mathbf{C}}^T & \tilde{\mathbf{H}}/\omega^2 - \tilde{\mathbf{Q}} \end{bmatrix}}_{\tilde{\mathbf{S}}(\omega)} \underbrace{\begin{Bmatrix} \{\mathbf{u}\} \\ \{\mathbf{P}\} \end{Bmatrix}}_{\tilde{\mathbf{X}}(\omega)} = \underbrace{\begin{Bmatrix} \tilde{\mathbf{F}}_{\mathrm{u}} \\ \tilde{\mathbf{F}}_{\mathrm{P}}/\omega^2 \end{Bmatrix}}_{\tilde{\mathbf{F}}} \tag{4}$$

where $\tilde{(\cdot)}$ denotes the complex-valued nature of its argument. The expressions for the state matrices $\tilde{\mathbf{K}}$, $\tilde{\mathbf{M}}$, $\tilde{\mathbf{H}}$, $\tilde{\mathbf{Q}}$ and $\tilde{\mathbf{C}}$ are functions of the topological design/decision variables $\boldsymbol{\chi}$. The construction of these matrices are explained by Atalla *et al.*[41] and will not be detailed here. $\{\mathbf{u}\}$ and $\{\mathbf{P}\}$ denote the solid phase displacement and fluid phase pressure degrees of freedom in the poroelastic system respectively. The associated global stiffness matrix $\tilde{\mathbf{S}}(\omega)$ and the load vector $\tilde{\mathbf{F}}$ are iteratively assembled over each angular frequency $\omega = 2\pi f$ to yield a system of linear equations. These equations are solved as given in Eq. (5) to obtain the solution vector $\tilde{\mathbf{X}}(\boldsymbol{\chi}, \omega)$ which will contain the displacement and pressure fields of the solid and fluid parts of the poroelastic material respectively.

$$\{\tilde{\mathbf{X}}(\boldsymbol{\chi}, \omega)\} = [\tilde{\mathbf{S}}(\boldsymbol{\chi}, \omega)]^{-1}\{\tilde{\mathbf{F}}\} \tag{5}$$

For normal incidence, assuming plane waves, the sound absorption coefficient can be computed using the two-microphone method. Considering two closely spaced points x_1 and x_2 in the air region, the complex pressure amplitudes in frequency domain P_{x_1} and P_{x_2} can be obtained from $\{\mathbf{P}\}$ in $\tilde{\mathbf{X}}$. The plane wave reflection coefficient $\tilde{R}_c$ can then be computed from these pressures as,

$$\tilde{R}_c(\boldsymbol{\chi}, \omega) = \frac{P_{x_1}(\boldsymbol{\chi}, \omega)e^{(-ikx_2)} - P_{x_2}(\boldsymbol{\chi}, \omega)e^{(-ikx_1)}}{-P_{x_1}(\boldsymbol{\chi}, \omega)e^{(ikx_2)} + P_{x_2}(\boldsymbol{\chi}, \omega)e^{(ikx_1)}} \tag{6}$$

Here, k is the wave number given by ω/c_{air} with c_{air} being the speed of sound in air. The sound absorption coefficient α is then given by:

$$\alpha(\boldsymbol{\chi}, \omega) = 1 - |\tilde{R}_c(\boldsymbol{\chi}, \omega)|^2 \tag{7}$$

The analytical gradient of absorption can be computed by using chain rule following a similar procedure to that of Lee *et al.*[24] From Eq. (7):

$$\frac{\partial \alpha}{\partial \chi_i} = -2|\tilde{R}_c|\frac{\partial |\tilde{R}_c|}{\partial \chi_i} \tag{8}$$

$$\frac{\partial |\tilde{R}_c|}{\partial \chi_i} = \frac{\Re(\tilde{R}_c \times \overline{\frac{\partial \tilde{R}_c}{\partial \chi_i}})}{|\tilde{R}_c|} \tag{9}$$

Eq. (9) computes the derivative of absolute of the complex-valued $\tilde{R}_c$, $\Re(\cdot)$ is the real part and $\overline{(\cdot)}$ is the complex conjugate operator. The gradient $\frac{\partial \tilde{R}_c}{\partial \chi_i}$ is obtained from $\frac{\partial P_{x_1}}{\partial \chi_i}$ and $\frac{\partial P_{x_2}}{\partial \chi_i}$, which in-turn are two elements from the derivative vector $\frac{\partial \tilde{\mathbf{X}}}{\partial \chi_i}$. To find $\frac{\partial \tilde{\mathbf{X}}}{\partial \chi_i}$, Eq. (5) is differentiated to get the following expression.

$$\frac{\partial}{\partial \chi_i}\tilde{\mathbf{X}}(\boldsymbol{\chi}, \omega) = [\tilde{\mathbf{S}}(\omega)]^{-1}\frac{-\partial[\tilde{\mathbf{S}}(\omega)]}{\partial \chi_i}\tilde{\mathbf{X}} \tag{10}$$

The above step involves a large matrix inversion followed by sparse matrix and vector multiplications repeated for each element in the design domain. This step is performed efficiently by using the adjoint-based approach as detailed by Lee, Göransson and Kim.[28] Since only two elements in $\frac{\partial \tilde{\mathbf{X}}}{\partial \chi_i}$ i.e., $\frac{\partial P_{x_1}}{\partial \chi_i}$ and $\frac{\partial P_{x_2}}{\partial \chi_i}$ need to be computed to compute the gradients, one can premultiply Eq. (10) by the term $\frac{\partial P_{x_1}}{\partial \mathbf{X}}$, which is a vector of 0s except for one element with a value of 1 corresponding to the P_{x_1} degree of freedom in Eq. (10.)

$$\begin{aligned} \frac{\partial P_{x_1}}{\partial \chi_i} &= \left(\frac{\partial P_{x_1}}{\partial \mathbf{X}}\right)^T \frac{\partial \tilde{\mathbf{X}}}{\partial \chi_i} \\ &= \left(\frac{\partial P_{x_1}}{\partial \mathbf{X}}\right)^T [\tilde{\mathbf{S}}]^{-1}\frac{-\partial[\tilde{\mathbf{S}}]}{\partial \chi_i}\tilde{\mathbf{X}} = \lambda_{x_1}^T \frac{-\partial[\tilde{\mathbf{S}}]}{\partial \chi_i}\tilde{\mathbf{X}} \end{aligned} \tag{11}$$

Then, one can find a fictitious response vector $\lambda_{x_1} = [\tilde{\mathbf{S}}]^{-1}\frac{\partial P_{x_1}}{\partial \mathbf{X}}$ and compute $\frac{\partial P_{x_1}}{\partial \chi_i}$ for each i by computing $\lambda_{x_1}^T\left(\frac{-\partial[\tilde{\mathbf{S}}]}{\partial \chi_i}\tilde{\mathbf{X}}\right)$ quickly. This avoids solving system of equations repeatedly for each element or performing explicit matrix inversions. The above step is crucial for speeding-up gradient methods. In addition to solving $[\tilde{\mathbf{S}}(\omega)]^{-1}\tilde{\mathbf{F}}$, two additional instances of solving system of equations is involved in finding λ_{x1} and λ_{x2}. Assuming all other steps are time insignificant, function evaluation with gradients are approximately three times as expensive as evaluating without gradient.

This procedure has to be repeated at each frequency ω and for fine frequency steps, the calculation could become expensive. Although not implemented in this work, it is worth noting that there exist various expansion methods[50–52] to speed up the computation for broad frequency range problems.

Further, the gradients $\frac{-\partial[\tilde{\mathbf{S}}]}{\partial \chi_i}$ are obtained by applying chain rule up to the material properties $(E, \nu, \widetilde{\rho}, \widetilde{\gamma}_s, \widetilde{\rho}_{eq}, \widetilde{\mathrm{K}}_{eq})$ which depend on the design variables $\boldsymbol{\chi}$.

C. Benchmark problem instances

For comparing the performance of various optimisation approaches, seven benchmark problem instances with different characteristics as given in Table I are utilised. A two-dimensional finite element model of a small rectangular unit cell of an absorbing wall, as shown in Fig. 1 is considered. The unit cell's dimensions, its discretisation into finite elements, the base porous material to fill the elements, and target frequencies to be absorbed vary for each problem instance.

The unit cell of height d is backed by a rigid wall on the right, and a normal incidence sound source is mod-

TABLE I. Benchmark problem instances (see section II C)

No.	Problem instance name	Mesh size nelx × nely	Length D (m)	Height d (m)	f_{min} Hz	f_{step} Hz	f_{max} Hz	Material ID (see Table II)
1	LKKK material broadband coarse-mesh	10 × 10	0.135	0.054	100	100	1500	1
2	Melamine - building problem	15 × 10	0.045	0.1	100	100	1500	2
3	High resistivity foam - low frequency	10 × 10	0.1	0.1	50	50	500	3
4	Melamine - automotive problem	10 × 10	0.02	0.1	100	100	1500	2
5	Melamine - high frequency problem	10 × 10	0.02	0.1	2000	1000	5000	2
6	Melamine -broadband fine-mesh	50 × 20	0.135	0.054	100	100	1500	2
7	Melamine -single target frequency	10 × 5	0.135	0.054	500	500	500	2

TABLE II. Acoustic and elastic properties of materials used in the benchmark problems in Table I. Here, ϕ is the open porosity, Λ' is the thermal characteristic length, Λ is the viscous characteristic length, σ is the static airflow resistivity, α_∞ is the tortuosity, k_0' is the thermal permeability, ρ is the bulk density, E is the solid elastic modulus, ν is the Poisson's ratio and η is the dissipation factor.

Material parameters	Material-1	Material-2	Material-3
Material:	LKKK[24]	Melamine	High-resistivity soft foam
Acoustic model:	JCAL	JCAL	JCAL[46–48]
ϕ	0.9	0.99	0.8
Λ' (μm)	449	196	100
Λ (μm)	225	98	10
σ (N·s·m^{-4})	25000	10000	300000
α_∞	7.8	1.01	3
k_0'	4.75e-09	4.75e-09	4.75e-09
ρ (kg·m^{-3})	31.08	8	80
E (Pa)	800000	160000	30000
(ν)	0.4	0.44	0.44
(η)	0.265	0.1	0.01

elled at the left end. A region from the rigid wall up to a length D is designated as the design domain. The design domain is followed by a fixed domain, which is just an air region in this case with a length L. The design domain is discretised into *nelx* and *nely* finite elements along the horizontal and vertical directions respectively. Within the unit cell, symmetry is assumed about the central horizontal line, and sliding boundaries (u_x-free, $u_y = 0$, P-free) are assumed at the top and bottom edges. To save computational effort, only half of the system is modelled, and symmetry is imposed about the centerline (u_x-free, $u_y = 0$, P-free). It has been verified that this gives the same absorptions as obtained when modelling the full unit cell with sliding supports in the top and bottom edges. In all the problem instances, the mean sound absorption coefficient under normal incidence across the target frequencies is to be maximised.

Although meant to be arbitrary, the problem instances are chosen from practical engineering examples. The material used for optimisation for each problem instance is picked from three choices in Table II. In problem instance 1, a special material previously used by Lee, Kim, Kim, and Kang[24] (LKKK material) is used on a coarser 10 × 10 discretisation. Note that the LKKK material may not representative of a physical material due to the high tortuosity value of 7.8. Problem instance 2 features a 45 mm long design domain representative of a typical building application. Problem instance 3 uses an artificial material with a high static airflow resistivity. In problem instance 4, a thin design domain of 2 cm, representative of a foam layer in an automotive absorber, is considered. In problem instance 5, a thin layer is optimised for high-frequency absorption. Among the problem instances, problem instance 6 has a relatively fine mesh size with 50 × 20 elements featuring a thicker design domain optimised on a broad frequency range. Other than 1 and 3, all problem instances use Melamine foam for control. In problem instance 7, a single target frequency is considered.

III. OPTIMISATION APPROACHES

Several gradient-free heuristic and metaheuristic approaches, including well known and novel, are evaluated in this study alongside the state-of-the-art gradient-based approach SIMP. Henceforth in this paper, all the heuristic and metaheuristic approaches will be referred to as *algorithms*, and they are not to be confused with *exact* algorithms as used by some authors. The algorithms tested and their settings are summarised in Table III.

Five heuristic algorithms namely HC, CH1, CH2, SIMPf0 and SIMPf2 are tested. HC is a first-improvement hill climbing, where each element is flipped between air and porous material, and the new solution is accepted if it is improving. Consecutive elements are flipped like in a raster scan (row-by-row) until the function evaluation budget is used up. CH1 is a constructive heuristic that starts from an air-filled solution and progressively adds porous material in elements of best improvement in absorption. Similarly, CH2 starts from a

TABLE III. Optimisation approaches tested (pseudocodes are included in the supplementary material).[60]

Abbr.	Optimisation approach	Procedure and parameter settings	Algorithm type: Deterministic or Non-deterministic	Trials	Search space	Gradient usage	Fn. eval. budget
		HEURISTICS					
HC	Hill climbing (first improvement)	Start with a random binary array solution; Bit flip the consecutive elements; Accept if improving and move to the next element; Repeat from the start unless fn. eval. budget is used up. Element ordering is like in a raster scan.	Non-deterministic since starting solution is random	31	Discrete	No	4096
CH1	Constructive heuristic: material addition	Start with air-filled design domain; Compute absorption improvement at each element by filling porous material only in that element; Sort elements; Add porous material at best 'm' improving elements; Repeat until design domain is fully porous; Track and return the best solution. m is chosen such that the budget is not exceeded.	Deterministic	1	Discrete	No	4096
CH2	Constructive heuristic: material removal	Similar to CH1. Start from fully porous design domain; Remove porous (replace with air) at 'm' least worsening elements; Repeat until all porous is removed; Track and return the best solution	Deterministic	1	Discrete	No	4096
SIMPf0	SIMP with no filter[53]	Start from a random continuous solution, follow the SIMP procedure[53]; Omit the filtering step. Use SIMP penalty $p = 3$; move update - optimality criteria; move limit $m = 0.2$; Volume fraction limit $V_f = 1$.	Non-deterministic	31	Continuous	**Yes**	1366
SIMPf2	SIMP with density filter[53]	Start from a random continuous solution, follow the SIMP procedure[53]; use density filter `ft=2`. Use SIMP penalty $p = 3$; move update - optimality criteria; move limit $m = 0.2$; Volume fraction limit $V_f = 1$; Filter radius r_{min} =2.	Non-deterministic	31	Continuous	**Yes**	1366
		METAHEURISTICS					
GA	Genetic algorithm[54]	Initialise population with 64 random binary solutions; Selection: tournament–2; Crossover: uniform; Mutation: bitflip; Mutation rate: 1/(N); Replacement: best of parents and offspring replace parents; Repeat from selection, unless budget is used up.	Non-deterministic (uses a random number generator)	31	Discrete	No	4096
TABU	Tabu search[55]	Initiate tabu list; Start with a random binary array solution; Pick a random bit, not in tabu list; Accept if improving and add the bit to tabu list; tabu tenure: 20% of N; Pick another random bit and repeat unless budget is used up.	Non-deterministic (since starting solution and moves are random)	31	Discrete	No	4096
CMA	Covariance-matrix-adaptation evolution strategy[56]	Relax problem to continuous using SIMP interpolation scheme with $p = 3$; Follow CMA procedure[56]; Terminate if budget is used up; Discretise final continuous solution by rounding.	Non-deterministic (uses a random number generator to sample points from the distribution)	31	Continuous	No	4096
CMAd	Discrete variant of CMA	Follow CMA procedure in continuous space; Before fitness evaluation, discretise the sampled continuous solutions by rounding; Return the rounded best solution. An interpolation scheme is not necessary as continuous solutions are never evaluated.	Non-deterministic	31	Discrete	No	4096
DE	Differential evolution[57,58]	Relax problem to continuous using SIMP interpolation scheme with $p = 3$; Follow differential evolution procedure[57,58]; Stop if budget is used up. Use population size=32; F=0.2; CR=0.2;	Non-deterministic	31	Continuous	No	4096
DEd	Discrete variant of DE	Follow the differential evolution procedure; Before fitness evaluation, discretise the sampled continuous solutions by rounding; Return the rounded best solution.	Non-deterministic	31	Discrete	No	4096

porous material-filled solution and progressively removes porous material from the elements where the decrease in absorption is the least. SIMPf0 and SIMPf2 are solid-isotropic-material-with-penalisation approaches[53] which use gradients of absorption to modify the solution at each step. While SIMPf2 uses density filtering, SIMPf0 uses no filtering techniques.

Four popular metaheuristic approaches are tested, including genetic algorithm (GA), tabu search (TABU), covariance-matrix-adaptation evolution strategy (CMA) and differential evolution (DE). Additionally, discrete variants of CMA and DE referred to as CMAd and DEd are also tested, where the continuous shapes are rounded before every absorption evaluation.

Except for CH1 and CH2, all the other algorithms are non-deterministic as they embed a random component, and each new trial of the non-deterministic algorithm could produce a different near-optimal solution. For these algorithms, 31 trials were run on each problem instance in order to assess their average performance and carry out statistical analyses.

All non-gradient algorithms are allowed 4096 function evaluations during the trials. Since absorption+ gradient evaluations take approximately thrice the computational time (Eq. 11), SIMPf0 and SIMPf2 are allowed 1366 function evaluations.

The discrete algorithms, which only allow air or porous elements in the design domain, are initiated from random discrete solutions with equal probability of air or porous material for each element (except for CH1 and CH2). The continuous algorithms, which allow intermediate materials between air and porous materials in each element, are initiated from solutions generated by assigning a random number uniformly distributed between 0 and 1 to the topological design variables. Such random initialisation is done to ensure a fair comparison making no a priori assumptions about the solution.

Some of the newly proposed approaches, namely, hill climbing, constructive heuristics, and the discrete variants of CMA evolution strategy and differential evolution, in the specific way used here are tested for the first time in topology optimisation. The others are well-established algorithms, and resources including surveys, tutorials and code implementations can be easily reached. More specific implementation details are included in the supplementary material. It is noted that a thorough knowledge of all the algorithms is not essential to understand the findings. These algorithms can be thought of as black-boxes that optimise the shape design by searching for the optimal assignment of the decision variables $\boldsymbol{\chi}$ to maximise $\overline{\alpha}(\boldsymbol{\chi})$.

IV. RESULTS AND DISCUSSION

A. Run time performance comparison

One of the desired aspects of a good topology optimisation strategy is the ability to find better quality solutions in a limited CPU time. As more CPU time is allowed, the algorithms progressively find solutions with higher absorption. Fig. 2(a) compares the progress of the best-so-far absorption values ($\overline{\alpha}$) obtained versus CPU time used by various algorithms on problem instance 6.

Multiple machines were used to run the optimisation tests, and in order to remove the machine-dependence on runtime in Fig. 2(a), the best-so-far absorption values were tracked against the number of function evaluations, and runtimes were then computed by using average time-per-function-evaluation clocked on a reference machine. The reference machine used features an Intel(R) Core(TM) i7-3820 CPU 3.6 GHz processor, 32 GB RAM and a 64-bit Windows 10 operating system running Matlab2019b[59]. Scales indicating the number of function evaluations are also provided for benchmarking purposes. For all non-deterministic algorithms, as multiple trials were conducted, the absorption values shown in Fig. 2(a) are averaged across the 31 trials after each generation of the algorithm.

First, note that initial absorption levels are different for the algorithms. While the discrete algorithms HC, GA, TABU, CMAd and DEd are initiated from random discrete solutions with $\overline{\alpha}$ around 0.71, the continuous algorithms CMA, DE, SIMPf0 and SIMPf2 are initiated from random continuous solutions with $\overline{\alpha}$ around 0.65. CH2 starts from fully porous design domain with $\overline{\alpha}$ around 0.84 and CH1 starts from an empty (air-filled) design domain with no absorption.

One of the first things to note is that the CH2 algorithm does not produce an improvement from the fully porous-filled solution and hence the best-so-far absorption value stays the same for this problem. For low CPU-time budgets, SIMPf0 and SIMPf2 produce higher quality solutions than all the other algorithms except CH2. SIMPf0 and SIMPf2 converge to a higher absorption than the porous-filled CH2 solution in under 5 min on this problem instance highlighting that gradient-based methods can be time-efficient. After about 20 min of runtime, HC produces better solutions on average than SIMP, but the difference is small.

After the designated budget of 4096 function evaluations (1366 gradient-included function evaluations), HC, SIMPf2, TABU, SIMPf0 and CH1 produce the top tier solutions. CMAd follows closely by producing slightly better-quality solutions compared to fully filled CH2 solution towards the end. Whereas for DEd and GA, the runtime performance was considerably poor.

It is important to appreciate that the solutions from continuous algorithms (CMA, DE, SIMPf0 and SIMPf2) consider intermediate materials between the porous material and air $\chi_i \in (0, 1]$ whereas the discrete algorithms consider only porous material or air solutions $\chi_i \in \{0, 1\}$. Since the solutions are from different search spaces, the absorption levels cannot be directly compared between the two. Although, the final shapes from continuous algorithms are desired to be 0 or 1, they are often not. Hence, they are forced to be discrete using a simple round-off filter, and the absorption values are recomputed. Such rounding leads to a drop or surge in the absorption values at the end of all continuous algorithms as can be observed noticeably in CMA and DE plotlines in Fig. 2(a). The rounded absorptions indicated by the end markers are also trial-averaged. Rounding leads to no significant changes in SIMPf0 and SIMPf2 solutions for this problem instance. For CMA and DE, the rounded solution absorption values were poorer than SIMP solutions.

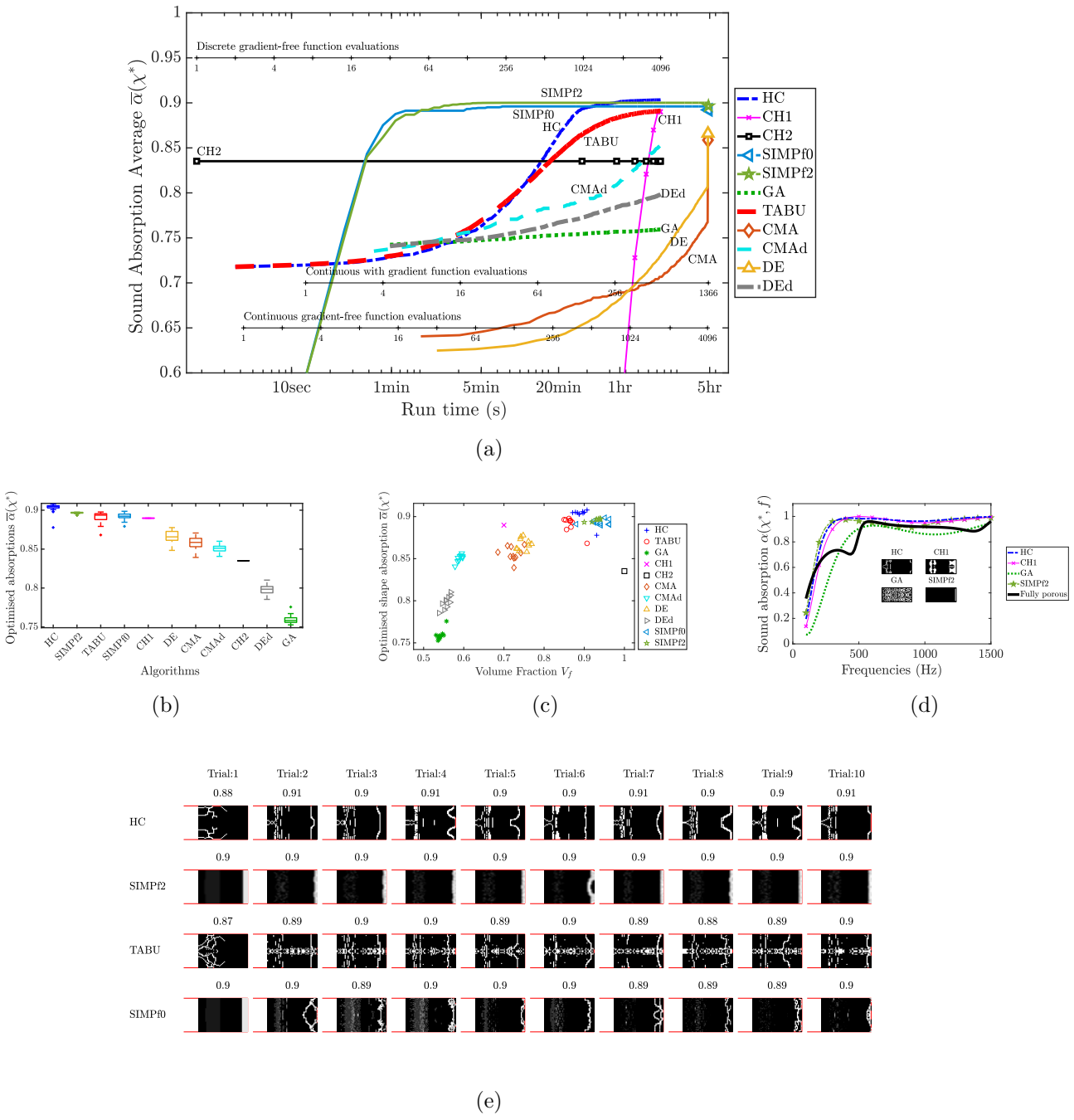

FIG. 2. (color online) Optimisation trials on problem instance 6: (a) Progress of best absorption found vs runtime (trial-averaged). For continuous algorithms, the solutions are discretised in the end. (b) Distribution of final solution absorption across trials. (c) Distribution of solution quality vs volume fraction (d) Sound absorption vs frequency for final shapes from select algorithms. (e) Best shapes from different trials from top four algorithms and their absorption.

The above behaviour of continuous algorithms does not seem to be the general trend across all problem instances. When considering the runtime performance of problem instance 1 shown in Fig. 3, SIMP algorithms produce final solutions with intermediate materials which when rounded result in a significant reduction in absorption. This behaviour is also prominent in other problem instances especially the one with the high resistivity material (plots for other problem instances included in the supplementary material).

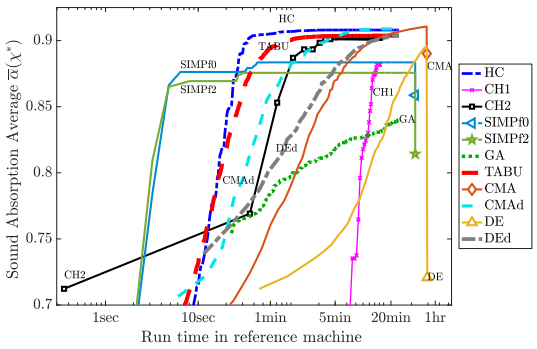

FIG. 3. (color online) Progress of best absorption found vs runtime: problem instance 1.

B. Final solution quality comparison

After rounding the continuous algorithm solutions and re-evaluating absorption, the distribution of final absorption values are shown in Fig. 2(b). What is interesting to note is that for non-deterministic algorithms, the 31 trials do not necessarily result in the same optimised shapes and the final absorption values are spread out. The boxes enclose first to third quartiles (i.e., 25 percentile to 75 percentile), the whiskers denote the span, and the crosses denote the outliers.

Often in practice, a particular topology optimisation strategy may be chosen, and one trial may be run to determine a near-optimal shape. In such cases, it is desirable to pick an algorithm that has the best median performance across trials. Hence, using the median absorption across trials, the algorithms are sorted best to worst from left to right in Fig. 2(b). HC and SIMPf2 turn out to be the top-performing algorithms for this problem instance followed by TABU, SIMPf0 and CH1 in the second tier. DE, CMA and CMAd follow with all trials producing better solutions than the fully-filled CH2 solution. DEd and GA performed the poorest with no trials producing better than the fully-filled solution.

The shapes produced from 10 of the trials from the top four algorithms are displayed in Fig. 2(e). Most shapes seem to have a thin layer of air near the rigid backing as this allows removing elastic resonance around 500 Hz as can be observed from the absorption curves in Fig. 2(d). Without filtering, SIMPf0 produces intricate designs near this thin air layer compared to SIMPf2.

C. Performance across problem instances

For an overall comparison, the ranking is extended to other problem instances in Table IV. Such a comparison across many problem instances is essential as algorithms performing well on one problem instance need not necessarily perform well on other problem instances. The ranking scheme is such that if the median absorption values of two or more algorithms are the same correct to two decimal places, they are assigned the same rank.

TABLE IV. The algorithms are ranked based on median values of optimised shape absorption ($\overline{\alpha}*$) across trails. Lesser the average rank, the better is the performance of the algorithm. Algorithms are sorted based on the average of the ranks across problem instances. This ranking scheme is provided for a quick look up only and is not meant to be a precise indicator of the performance. The ranking could change if more problem instances and algorithms are considered.

Ranks	Problem instances →							Avg. rank
Algorithms ↓	1	2	3	4	5	6	7	
HC	**1**	**1**	3	**1**	**1**	**1**	**1**	**1.29***
CMAd	**1**	3	**1**	**1**	4	8	**1**	2.71
CH1	7	**1**	8	**1**	**1**	3	**1**	3.14
TABU	**1**	5	4	8	7	3	**1**	4.14
CH2	5	6	4	**1**	4	9	**1**	4.29
SIMPf0	8	3	10	**1**	4	3	9	5.43
SIMPf2	10	6	11	**1**	**1**	**1**	11	5.86
DEd	**1**	9	2	10	9	10	**1**	6
CMA	6	6	4	8	9	7	8	6.86
DE	11	11	9	**1**	7	6	9	7.71
GA	9	10	4	11	11	11	**1**	8.14

This ranking is only provided for a quick summary of the optimisation tests, and it is emphasised that the ranks may not be the same for a different set of problem instances.

From Table IV, one can observe that HC, CMAd and CH1 rank among the top three. Although SIMPf2 and SIMPf0 performed well on problem instance 6, they take respectively the 6^{th} and 7^{th} places overall among the algorithms compared.

Surprisingly, the simple first-improvement hillclimbing (HC) ranks among the best in all problem instances except the high-resistivity material instance (problem instance 3). This means that HC's potential can to be exploited by using it in hybrid algorithms. It is worth noting that HC applied to the MBB beam compliance minimisation[6] results in the trivial fully-solid-filled solution. A simple way to avoid this is to use a volume fraction penalty with the objective function.

CMAd and CH1 ranked first in four problem instances. Although CMAd ranked 8^{th} in problem instance 6, its overall performance across the problem instances puts the algorithm in second place. Notably, in problem instance 3, which considers a high static airflow resistivity material, CMAd performed the best. This problem instance likely has many local optima and the performance of CMAd indicates its global topology optimisation potential. The poor performance of the SIMP algorithms in this problem instance is likely due to the multi-modality of the objective function and premature convergence to local optima.

Although the progress of absorption in the initial stages of CH1 is slow compared to the other algorithms, the final absorption value makes CH1 one of the best algorithms. Notably, for many problem instances considered, the best absorption value from CH1 is higher than the absorption of the discretised solutions from both SIMPf0 and SIMPf2. CH1 seems to be better overall compared to CH2, indicating that constructing the solution from scratch may be better than removing material from a fully-filled solution.

Performance of CMA and DE were relatively poor in this benchmark. One reason could be that the number of design variables is large and these strategies do not exploit the correlation of the neighbouring-element design variables, a special attribute in topology optimisation problems.

Both CMAd and DEd seem to perform better than CMA and DE in general, indicating that rounding during the algorithm may be a better approach than rounding the solutions after the termination of continuous algorithms. While CMAd ranked among the top, the performance of DEd was similar to that of SIMP in terms of solutions quality.

Among the algorithms considered, GA performed the poorest. Though, scope for improvement exists in terms of using better mutation and crossover operators adapted to topology optimisation, focus may be diverted to other strategies which show better promise.

D. Best shapes obtained from algorithms

The best solutions from all the algorithms for all problem instances are plotted in Fig. 4. For non-deterministic algorithms, the solution with the highest absorption among the 31 trials is shown. It is recalled that manufacturability restrictions and morphological filters are not imposed in this study except for SIMPf2. Results show both SIMPf0 and SIMPf2 produce similar shapes for most problem instances.

For problem instance 1, all algorithms except SIMPf2 result in irregular shapes. The best quality shapes from most algorithms are flat layers of air and porous material towards the rigid wall with a somewhat circular air cavity in the front. GA and DE produced checkerbox shapes. Moreover, shapes from GA for all problem instances are degenerate.

For problem instance 2, HC, CH1 and SIMPf0 produce the best shape with an almost porous material filled design domain except for a layer of air next to the rigid wall. CH1, SIMPf2, CMA, CMAd, TABU produced similar shapes. CH2 resulted in a fully-filled shape with slightly less absorption.

In problem instance 3 with a high static airflow resistivity material, the shapes from all algorithms were seemingly random patterns but with sort of a cavity in the centre. SIMPf2 produces a result with a chunk of porous material suspended in the air.

For problem instance 4, the optimal solution seems to be a fully-filled design domain and most algorithms are able to find this except for GA. The reason could be that GA is initiated from random bit arrays which would have volume fraction distributed near 50 % (central limit theorem). Thus, initialising GA with solutions with a range of volume fractions might be a sounder approach.

For problem instance 5, many algorithms find a solution with a shape almost filled with the porous material except for air pockets near the rigid wall. CMA, DE and DEd seem to be approaching this solution. CH2 completely fills the design domain with the porous material.

For problem instance 6, the fully-filled solution has an elastic resonance in the frequency range considered, as may be seen from Fig. 2(d). The elastic resonance forms a drop in the absorption near 500 Hz. The best solutions from different algorithms effectively remove this resonance. To do this, the algorithms seem to introduce air layers at the front and near the rigid backing. CMA, CMAd, DE and DEd give checker-board shapes which somewhat removes a layer near the rigid backing. Notably, CH1 gives a smooth shape even though no manufacturability restrictions were imposed. CH2 returns a filled design domain and is unable to get rid of the resonance.

For problem instance 7, many solutions have close to complete sound absorption ($\overline{\alpha} = 1$). Almost all algorithms find solutions with total sound absorption at 500 Hz. Notably, SIMPf0 and SIMPf2 seem to suggest a fully-filled solution.

In general, the algorithms which feature random move operations tend to produce degenerate shapes. Although hill climbing results in shapes with high sound absorption, the shapes obtained are sometimes irregular and need additional filtering. On the other hand, constructive heuristic with material addition (CH1) has both high performance and finds shapes with smoother boundaries.

In summary, different algorithms seem to provide solutions from a unique pool (Fig. 2(c)). The reason for this is each approach uses unique move operations during the optimisation to reach solutions that may not be explored by other algorithms. Thus it may be worth many optimisation strategies to find a set of unique solutions which may be of interest to the acoustic engineer. In addition, scope for improving many of these methods exist. As an example, the performance of SIMP could be improved by using better strategies for avoiding local optima, and an appropriate morphological filter may be used in CMAd to overcome the drawback of producing unconnected shapes while speeding up the algorithm. The results outlined in this article provides an initial understanding of various heuristics and metaheuristics perform on topology optimisation for absorption maximisation. Thus, guidelines for developing hybrid algorithms and hyper-heuristics may be arrived at for devising more time-efficient strategies that also produce solutions closer to the true optima.

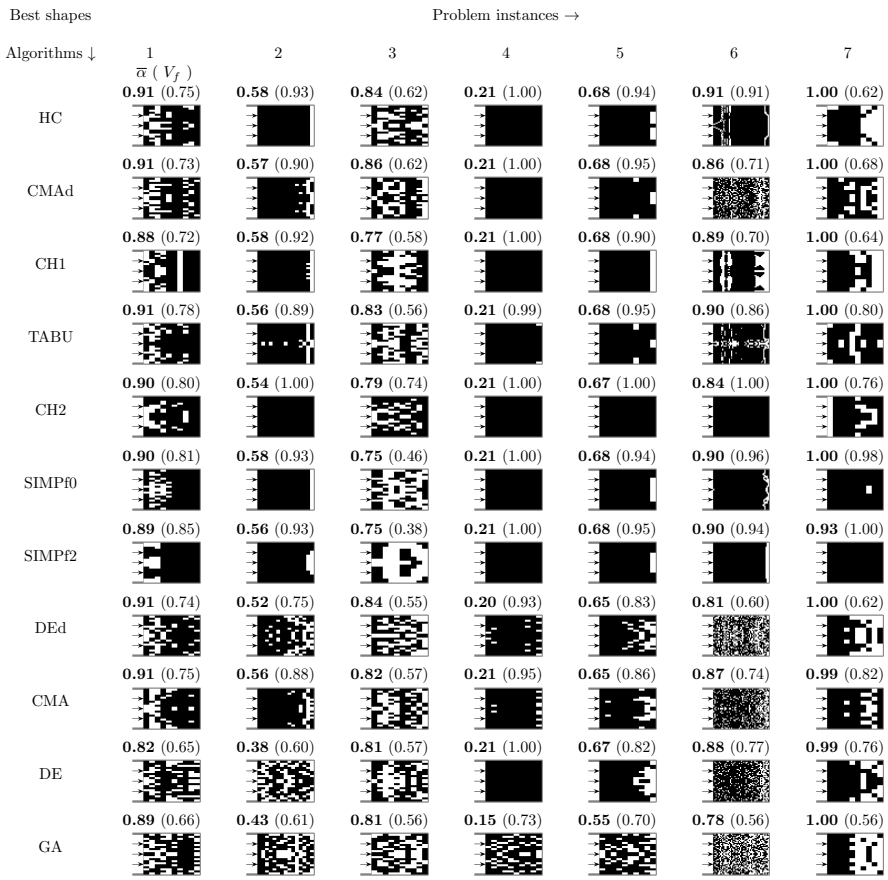

FIG. 4. Optimised shapes obtained from all algorithms for each problem instance. The shapes are discretised by rounding for continuous algorithms. The values of mean absorption across frequencies ($\overline{\alpha}$) are printed at the top of each shape in bold font along with porous material volume fraction (V_f) in parentheses. White and black represent air and the porous, respectively, with the acoustic input on the left and rigid backing on the right.

V. CONCLUSIONS

In this work, topology optimisation to maximise sound absorption under normal incidence in an impedance tube with a rigid backing is considered. Optimisation tests were conducted using 5 heuristic and 6 metaheuristic algorithms on 7 benchmark problem instances. The approaches include hill climbing (HC), constructive heuristics (CH1 and CH2), solid-isotropic-material-with-penalisation (SIMPf0 and SIMPf2), genetic algorithm (GA), tabu search (TABU), covariance-matrix-adaptation evolution strategy (CMA and CMAd), and differential evolution (DE and DEd). Unlike in usual structural topology optimisation problems, volume fraction constraint and manufacturability filters were not imposed. The highlights of the findings are as follows.

- Gradient algorithms (SIMPf0 and SIMPf2) can quickly converge to good quality solutions, but in some problems, they either prematurely converge to local optima or produce shapes that have intermediate materials indicating that the objective function is multimodal with many local optima.

- When comparing the solution quality, no algorithm clearly outperformed all others on all of the problem instances. Ranking the algorithms based on median solution quality revealed that the hill climbing approach performed the best, followed by the material-addition constructive heuristic (CH1), and the discrete variant of covariance-matrix-adaptation evolution strategy (CMAd).

- The optimal shapes produced by algorithms that use stochastic components (GA, CMA, CMAd, DE, DEd) tend to be irregular and unconnected, and hence they might need additional filtering techniques. Although HC produced higher sound absorption solutions in general, the optimal shapes

produced were not smooth and crisp. On the other hand, CH1 produces high-quality solutions that also have fewer irregularities than HC. In addition to this, the sound absorption values of shapes produced by CH1 were as good as or slightly better than those produced by SIMPf0. Moreover, CH1 can be easily modified to include volume fraction constraint by terminating the construction after the desired volume fraction is reached. The material removal heuristic (CH2) often returns a fully filled design domain as the solution, and the reason for this is not clear.

- Between the continuous algorithms (CMA and DE) and their discrete variants (CMAd and DEd), the discrete variants seem to perform better. This means using filtering techniques before each objective function evaluation works better than filtering the solutions at the end of the algorithm.

To conclude, the absorption maximisation topology optimisation problem seems to be rich with many local-optimal solutions, and different strategies explore different regions of the search space producing unique varieties of solutions. Insights obtained may be valuable in designing hybrid strategies and hyperheuristics for general-purpose optimisation of sound-absorbing materials.

ACKNOWLEDGEMENT

This work is part of a project that has received funding from the European Research Council (ERC) under the European Union's Horizon 2020 research and innovation programme *No2Noise* (Grant agreement No. 765472). The authors wish to thank the anonymous reviewers whose suggestions have greatly improved the manuscript.

[1]M. P. Bendsøe and N. Kikuchi, "Generating optimal topologies in structural design using a homogenization method", Comp. Meth. App. Mech. Eng., **71**(2), 197–224, (1988).

[2]M. Stolpe and M. P. Bendsøe, "Global optima for the Zhou–Rozvany problem", Struct. Multi. Optim., **43**(2), 151–164, (2011).

[3]M. Zhou and G.I.N Rozvany, "On the validity of ESO type methods in topology optimization", Struct. Multi. Optim., **21**(1), 80–83, (2001).

[4]M. P. Bendsøe, "Optimal shape design as a material distribution problem", Struct. Optim., **1**(4), 193–202, (1989).

[5]M. Zhou and G.I.N. Rozvany, "The COC algorithm, part ii: Topological, geometrical and generalized shape optimization", Comp. Meth. App. Mech. Eng., **89**(1-3), 309–336, (1991).

[6]O. Sigmund, "A 99 line topology optimization code written in Matlab", Struct. Multi. Optim., **21**(2), 120–127, (2001).

[7]Y. M. Xie and G. P. Steven, "A simple evolutionary procedure for structural optimization", Comp. & Struct., **49**(5), 885–896, (1993).

[8]Y. M. Xie and G. P. Steven, "Evolutionary structural optimization for dynamic problems", Comp. & Struct., **58**(6), 1067–1073, (1996).

[9]X. Y. Yang, Y. M. Xie, G. P. Steven, and O. M. Querin, "Topology optimization for frequencies using an evolutionary method", J. Struct. Eng., **125**(12), 1432–1438, (1999).

[10]M. Y. Wang, X. Wang, and D. Guo, "A level set method for structural topology optimization", Comp. Meth. App. Mech. Eng., **192**(1-2), 227–246, (2003).

[11]G. Allaire, F. Jouve, and A.M. Toader, "Structural optimization using sensitivity analysis and a level-set method", J. Comp. Physics, **194**(1), 363–393, (2004).

[12]M. Burger, B. Hackl, and W. Ring, "Incorporating topological derivatives into level set methods", J. Comp. Physics, **194**(1), 344–362, (2004).

[13]M. P. Bendsøe and O. Sigmund, *Optimization of structural topology, shape, and material*, Vol. 414 (Springer, New York, 1995).

[14]K. Svanberg, "The method of moving asymptotes—a new method for structural optimization", Int. J. Num. Meth. Eng., **24**(2), 359–373, (1987).

[15]F. Glover and M. Laguna, "Tabu search", In *Handbook of Combinatorial Optimization* (Springer, New York, 1998), pp. 2093–2229.

[16]D. Guirguis, N. Aulig, R. Picelli, B. Zhu, Y. Zhou, W. Vicente, F. Iorio, M. Olhofer, W. Matusik, C. A. Coell Coello, and K. Saitou, "Evolutionary black-box topology optimization: Challenges and promises", IEEE Trans. Evol. Comp.,**24**, 613-633 (2019).

[17]V. T. Ramamoorthy, E. Özcan, A. J. Parkes, Jaouen L., and F.-X. Bécot, "Acoustic topology optimisation using CMA-ES", in *Proceedings of ISMA2020 and USD2020* (2020), pp.511-522.

[18]M. P. Bendsoe and O. Sigmund, "*Topology optimization: theory, methods, and applications*", (Springer, New York, 2013).

[19]O. Sigmund and K. Maute, "Topology optimization approaches", Struct. Multi. Optim., **48**(6), 1031–1055, (2013).

[20]G.I.N Rozvany, "Aims, scope, methods, history and unified terminology of computer-aided topology optimization in structural mechanics. Struct. Multi. Optim., **21**(2), 90–108, (2001).

[21]J. D. Deaton and R. V. Grandhi, "A survey of structural and multidisciplinary continuum topology optimization: post 2000", Struct. Multi. Optim., **49**(1), 1–38, (2014).

[22]E. Wadbro and M. Berggren, "Topology optimization of an acoustic horn. Comp. meth. app. mech. eng., **196**(1-3), 420–436, (2006).

[23]M. B. Dühring, J. S. Jensen, and O. Sigmund, "Acoustic design by topology optimization", J. Sound Vib., **317**(3-5), 557–575, (2008).

[24]J. S. Lee, Y. Y. Kim, J. S. Kim, and Y. J. Kang, "Two-dimensional poroelastic acoustical foam shape design for absorption coefficient maximization by topology optimization method", J. Acous. Soc. America, **123**(4), 2094–2106, (2008).

[25]J. W. Lee and Y. Y. Kim, "Topology optimization of muffler internal partitions for improving acoustical attenuation performance", Int. J. Num. Meth. Eng., **80**(4), 455–477, (2009).

[26]J. Kook, K. Koo, J. Hyun, J. S. Jensen, and S. Wang, "Acoustical topology optimization for Zwicker's loudness model–application to noise barriers", Comp. Meth. App. Mech. Eng., **237-240**, 130–151, (2012).

[27]G. H. Yoon, "Acoustic topology optimization of fibrous material with Delany–Bazley empirical material formulation", J. Sound Vib., **332**(5), 1172–1187, (2013).

[28]J. S. Lee, P. Göransson, and Y. Y. Kim, "Topology optimization for three-phase materials distribution in a dissipative expansion chamber by unified multiphase modeling approach", Comp. Meth. App. Mech. Eng., **287**, 191–211, (2015).

[29]K. H. Kim and G. H. Yoon, "Optimal rigid and porous material distributions for noise barrier by acoustic topology optimization", J. Sound Vib., **339**, 123–142, (2015).

[30]E. L. Yedeg, E. Wadbro, and M. Berggren, "Interior layout topology optimization of a reactive muffler", Struct. Multi. Optim., **53**(4), 645–656, (2016).

[31]L. Chen, C. Liu, W. Zhao, and L. Liu, "An isogeometric approach of two dimensional acoustic design sensitivity analysis and topology optimization analysis for absorbing material distribution", Comp. Meth. App. Mech. Eng., **336**, 507–532, (2018).

[32]J. Kook, "Evolutionary topology optimization for acoustic-structure interaction problems using a mixed u/p formulation", Mech. Based Des. Struct. and Mach., **47**(3), 356–374, (2019).

[33]W. U. Yoon, J. H. Park, J. S. Lee, and Y. Y. Kim, "Topology optimization design for total sound absorption in porous media", Comp. Meth. App. Mech. Eng., **360**, 112723, (2020).

[34]Y. Xu, W. Zhao, L. Chen, and H. Chen, "Distribution optimization for acoustic design of porous layer by the boundary element method", Acous. Australia, **48**, 107–119, (2020).

[35]L. Chen, C. Lu, H. Lian, Z. Liu, W. Zhao, S. Li, H. Chen, and S. P. Bordas. "Acoustic topology optimization of sound absorbing materials directly from subdivision surfaces with isogeometric boundary element methods", Comp. Meth. App. Mech. Eng., **362**, 112806, (2020).

[36]Z.-X. Xu, H. Gao, Y.J. Ding, J. Yang, B. Liang, and J.-C. Cheng, "Topology-optimized omnidirectional broadband acoustic ventilation barrier", Phy. Rev. App., **14**(5), 054016, 2020.

[37]O. Sigmund and P. M. Clausen, "Topology optimization using a mixed formulation: an alternative way to solve pressure load problems. Comp. Meth. App. Mech. Eng., **196**(13-16), 1874–1889, 2007.

[38]G. H. Yoon, J. S. Jensen, and O. Sigmund, "Topology optimization of acoustic–structure interaction problems using a mixed finite element formulation", Int. J. Num. Meth. Eng., **70**(9), 1049–1075, 2007.

[39]P. Göransson, J. Cuenca, and T. Lähivaara, "Parameter estimation in modelling frequency response of coupled systems using a stepwise approach", Mech. Sys. Sig. Proc., **126**, 161–175, 2019.

[40]K. Svanberg, "A class of globally convergent optimization methods based on conservative convex separable approximations", SIAM J. Optim., **12**(2), 555–573, 2002.

[41]N. Atalla, R. Panneton, and P. Debergue, "A mixed displacement-pressure formulation for poroelastic materials", J. Acous. Soc. America, **104**(3), 1444–1452, 1998.

[42]F.-X. Bécot and L. Jaouen, "An alternative Biot's formulation for dissipative porous media with skeleton deformation", J. Acous. Soc. America, **134**(6), 4801–4807, 2013.

[43]H. Isakari, K. Kuriyama, S. Harada, T. Yamada, T. Takahashi, and Toshiro Matsumoto, "A topology optimisation for three-dimensional acoustics with the level set method and the fast multipole boundary element method", Mech. Eng. J., **1**(4), CM0039–CM0039, 2014.

[44]P. Rostami and J. Marzbanrad, "Identification of optimal topologies for continuum structures using metaheuristics: A comparative study", Arch. Comp. Meth. Eng., pages 1–28, 2021.

[45]M. Ranjbar, S. Marburg, and H.-J. Hardtke, "Structural-acoustic optimization of a rectangular plate: A tabu search approach", Finite elements in analysis and design, **50**, 142–146, 2012.

[46]D. L. Johnson, J. Koplik, and R. Dashen, "Theory of dynamic permeability and tortuosity in fluid-saturated porous media", J. Fluid Mech., **176**, 379–402, 1987.

[47]Y. Champoux and J.-F. Allard, "Dynamic tortuosity and bulk modulus in air-saturated porous media", J. App. Physics, **70**(4), 1975–1979, 1991.

[48]D. Lafarge, P. Lemarinier, J. F. Allard, and V. Tarnow, "Dynamic compressibility of air in porous structures at audible frequencies", J. Acous. Soc. America, **102**(4), 1995–2006, 1997.

[49]M. P. Bendsøe and O. Sigmund, "Material interpolation schemes in topology optimization", Arch. App. Mech., **69**(9-10), 635–654, 1999.

[50]M. Souza Lenzi, S. Lefteriu, H. Beriot, and W. Desmet, "A fast frequency sweep approach using padé approximations for solving helmholtz finite element models", Journal of Sound and Vibration, **332**(8), 1897–1917, 2013.

[51]R. Rumpler, P. Göransson, and H.J. Rice, "An adaptive strategy for the bivariate solution of finite element problems using multivariate nested padé approximants", International Journal for Numerical Methods in Engineering, **100**(9), 689–710, 2014.

[52]R. Rumpler, P. Göransson, and J.-F. Deü, "A finite element approach combining a reduced-order system, padé approximants, and an adaptive frequency windowing for fast multi-frequency solution of poro-acoustic problems", International Journal for Numerical Methods in Engineering, **97**(10), 759–784, 2014.

[53]E. Andreassen, A. Clausen, M. Schevenels, B. S. Lazarov, and O. Sigmund, "Efficient topology optimization in MATLAB using 88 lines of code", Struct. Multi. Optim., **43**(1), 1–16, 2011.

[54]J. H. Holland, *Adaptation in natural and artificial systems: an introductory analysis with applications to biology, control, and artificial intelligence*, MIT press, 1992.

[55]F. Glover, "Future paths for integer programming and links to artificial intelligence", Comp. & op. research, **13**(5), 533–549, 1986.

[56]N. Hansen, "The CMA evolution strategy: A tutorial", arXiv preprint arXiv:1604.00772, 2016.

[57]R. Storn, "On the usage of differential evolution for function optimization", in *Proceedings North American Fuzzy Information Processing*, pages 519–523. IEEE, 1996.

[58]R. Storn and K. Price, "Differential evolution–a simple and efficient heuristic for global", optimization over continuous spaces. J. Global Optim., **11**(4), 341–359, 1997.

[59]The MathWorks Inc., MATLAB version 9.7.0.1216025 (R2019b) Update 1.

[60]See suplementary material at https://www.scitation.org/doi/suppl/10.1121/10.0006784 for pseudocode and results for all problem instances.